A new fractal-theory-based criterion for hydrological model calibration

Zhixu Bai[1], Yao Wu[1], Di Ma[1], Yue-Ping Xu[1]

[1]Institute of Hydrology and Water Resources, Civil Engineering, Zhejiang University, Hangzhou, 310058, China

Correspondence to: Yue-Ping Xu (yuepingxu@zju.edu.cn)

Abstract. Fractality has been found in many areas and has been used to describe the internal features of time series. But is it possible to use fractal theory to improve the performance of hydrological models? This study aims at investigating the potential benefits of applying fractal theory in model calibration. A new criterion named ratio of fractal dimensions (RD) is defined as the ratio of fractal dimensions of simulated and observed streamflow series. To combine the advantages of fractal theory with classical criteria based on squared residuals, a multi-objective calibration strategy is designed. The selected classical criterion is Nash-Sutcliffe efficiency (E). The E-RD strategy is tested in three study cases with different climate and geography. The results of experiment reveal that, from most aspects, introducing RD into model calibration makes the simulation of streamflow components more reasonable. Besides, in calibration, only little decrease of E occurs when pursuing better RD. We therefore recommend choosing the best E among the parameter sets whose RD is around 1.

Key words: fractal theory; Hausdorff dimension; multi-objective calibration; hydrological model

1 Introduction

Since the first hydrological model was developed, proper methods to evaluate the performance of models have been pursued by hydrological community and a large variety of criteria have been proposed and used over the years. Most of the criteria are based on the squared residuals or absolute errors (Pushpalatha et al., 2012). Krause et al. (2005) compared nine efficiency criteria including correlation coefficient (r^2), Nash-Sutcliffe efficiency (E), index of agreement (d) and their variants, but none of them show overall dominance. Kling-Gupta efficiency was developed by Gupta et al. (2009) and Kling et al. (2012) to provide a diagnostically interesting decomposition of the Nash-

Sutcliffe efficiency, which facilitates the analysis of the relative importance of its different components (correlation, bias and variability) in the context of hydrological modelling. Apart from criteria which are used to calculate model errors over the entire test period, there are also many criteria which focus on a certain period of interest. For example, criteria mentioned above are calculated over flood periods

45 (Liu et al., 2017, 2019) or dry periods (Demirel et al., 2013). There are also studies which calibrated hydrological models over different hydrological components other than streamflow, such as evapotranspiration (Pan et al., 2017), soil moisture (Gao et al., 2015), snow water equivalent and even glacier melt (Liu et al., 2019). Another approach to improve the performance of models is the use of hydrological signature (Shafii and Tolson, 2015). Nonetheless, uncertainties of hydrological signature

50 simulation are often large (Westerberg and McMillan, 2015). Hao and Singh (2013) proposed a method based on entropy theory for constructing the bivariate distribution of drought duration and severity with different marginal distribution forms. Pechlivanidis et al. (2015) combined conditioned entropy difference metric and Kling-Gupta efficiency for multi-objective calibration of hydrologic models. Li et al. (2010) used the Bayesian method for uncertainty assessment of hydrological model

55 estimation.

Chiew and McMahon (1993) classified calibration criteria into statistical parameters and dimensionless coefficients. Statistical parameters include mean value, standard deviation, coefficient of skewness, coefficient of variance and quantile points etc. Most of the dimensionless coefficients (include Pearson correlation coefficient (r^2), Nash-Sutcliffe efficiency coefficient (E) and Kling-

60 Gupta efficiency coefficient etc.) are based on the squared residuals (Pushpalatha et al., 2012). According to squared-residuals-based coefficients' calculation formula, approaching of every simulated individual data to observed data makes the coefficients better.

Another deficiency of existing criteria is the preference of particular parts of hydrograph. For example, statistical parameters are easily influenced by extreme individuals and are with large uncertainties

65 (Westerberg and McMillan, 2015). Coefficients provide a measure of the overall agreement between simulation and observation, but are still significantly influenced by particular parts of hydrograph. High flows make a significant contribution to the value of E and Kling-Gupta efficiency coefficient (Pushpalatha et al., 2012). Nevertheless, former studies report an underestimation of peak flow when

2

删除了: s

删除了: (Liu et al., 2017; Liu et al., 2019)

删除了: (Demirel et al., 2013)

删除了: studies

删除了: (Pan et al., 2017)

删除了: (Gao et al., 2015)

删除了: (Liu et al., 2019)

删除了: modify

删除了: (Shafii et al., 2015)

删除了: (Westerberg and McMillan, 2015)

删除了: (

删除了: ,

删除了: Studies also used methods of loss function in model calibration. For example, Hao et al. (2013)

域代码已更改

删除了: (

删除了: ,

删除了: Pechlivanidis et al. (2014)

删除了: (

删除了: ,

删除了: Li et al. (2010)

域代码已更改

删除了: (

删除了: ,

移动了(插入) [3]

删除了: Chiew and McMahon (1993)

删除了: Dimensionless coefficients include Pearson correlation coefficient (r^2), Nash-Sutcliffe efficiency ... [1]

删除了: (Pushpalatha et al., 2012)

删除了: However, this doesn't make models more ... [2]

删除了: (Westerberg and McMillan, 2015)

删除了: (Pushpalatha et al., 2012)

删除了: literatures

using E as indicator alone (Jain and Sudheer, 2008). Overall, there is still large vacancy for calibration criteria which can give consideration to individual data and whole hydrograph.

Since firstly introduced by Hurst in 1951, fractality of streamflow series has been studied for decades (Hurst, 1951). There has been a spectacular growth in fractal theory, which was expended to various areas and to multifractal theory (Bai et al., 2019; Davis et al., 1994). Following the fractal theory, descriptions of fractality include the Hurst exponent (rescaled range analysis) (Hurst, 1951), Hausdorff dimension (box-counting dimension or local dimension) (Jelinek, 2008; Falconer, 2004), and correlation dimension (Grassberger and Procaccia, 1983) etc. The difference of these dimensions is the calculation scheme of fractal dimensions, and they are numerically related and theoretically dependent. While the Hurst exponent calculated with rescaled range analysis was more widely used, the Hausdorff dimension could be expanded to multifractal analysis easily and has perspective applications in hydrology (Bai et al., 2019; Zhou et al., 2014). The fractality of time series is generally considered as a reflection of self-affinity, periodicity, long-term memory and irregularity (Bai et al., 2019; Hurst, 1951; Mandelbrot, 2004). Self-affinity is a feature of a fractal whose pieces are scaled by different amounts in the x- and y-directions, and fractal dimensions represent the self-affinity of time series. The self-affinity of time series is the similarity of fine-resolution small parts and coarse-resolution large parts of data. Hausdorff dimension is defined and calculated based on the self-affinity of data series. The periodicity and long-term memory of time series referred by its fractality are highly related. Long-term memory is the feature that the effect of an event in a series may persist for a relatively long time. Long-term memory of hydrological time series is usually studied with rescaled range analysis. The irregularity of a fractal series refers to the unpredictable changes in a time series, which is a feature of chaos system. Generally, the Hausdorff dimension of streamflow series represents the magnitude of fluctuation, i.e., the fluctuations in river flow are large for large river flow and small for small river flow (Movahed and Hermanis, 2008). Such feature is also called as long-term correlation, which can be described with the Hausdorff dimension (Onyutha et al., 2019). However, applications of fractal theory in hydrology are limited in simple streamflow analysis, mostly only using the Hurst index (Katsev and L'Heureux, 2003). Also, some studies mentioned other indices based on fractal theory (Bai et al., 2019; Zhou et al., 2014; Zhang et al., 2010), but again, the research

3

删除了: (Jain and Sudheer, 2008)

删除了: Overall, there is still large vacancy for calibration criteria which can give consideration to individual data and whole hydrograph. ↵

删除了: (Hurst, 1951)

删除了: (Bai et al., 2019; Davis et al., 1994)

移动了(插入) [4]

删除了: (Hurst, 1951)

删除了: (Jelinek et al., 2008; Kenneth, 1990)

删除了: (Grassberger and Procaccia, 1983)

删除了: and of dependent significances theoretically

删除了: (Bai et al., 2019; Zhou et al., 2014)

删除了: (Bai et al., 2019; Hurst, 1951; Mandelbrot, 2004)

移动了(插入) [5]

删除了: (Movahed and Hermanis, 2008)

删除了: (Onyutha et al., 2019)

删除了: were

删除了: (Katsev and Lheureux, 2003)

删除了: literatures

删除了: indexes

删除了: (Bai et al., 2019; Yu et al., 2014; Zhang et al., 2010)

objects were only observed hydrological data. Recent studies made a progress to hydrological modelling based on fractal theory (Zhang et al., 2010), but the model only reconstructed flood/drought grades series. As demonstrated by all these studies, the fractality of observed streamflow series (as well as other hydro-meteorological data) is inherent and represents some peculiarity of their study cases. However, few studies have tried to explore the applications of fractal theory in hydrological model calibration. To our best knowledge, the only exception is Onyutha et al. (2019), who utilized the Hurst-Kolomogorov framework to evaluate the performance of climate models (GCM and RCM) rather than to calibrate hydrological models. In their study, the Hurst exponent was used to represent the long-range dependence and evaluate the reproductivity of variability (Onyutha et al., 2019). However, the benefits of using fractal theory in model building and calibration have not been discussed.

Unlike typical statistical evaluation of fluctuation (such as standard deviation and distribution function), the Hausdorff dimension takes the order of data into account. Therefore, on the basis of classical criteria who compare observed and simulated water balances, the Hausdorff dimension can offer useful insight into mechanisms controlling the extreme hydrological events (including floods, droughts and low flows) (Radziejewski et al., 1997). Another difference between fractal dimension and classical criteria is the influence of individual (or a small number of) data. While approaching of every simulated individual data to observed data makes the coefficient better, it may make the Hausdorff dimension of simulated data closer or farther away from that of observed data. That means, to reproduce all characteristics of observed streamflow, simulated streamflow and observed streamflow should have similar Hausdorff dimensions, as well as other traditional metrics. Given all that, the Hausdorff dimension is proposed in this study in hydrological model calibration.

Since the fractal dimension describes the fractality of streamflow series and two different series may have the same fractal dimension, the fractal dimension could not be used to calibrate hydrological model independently. Multi-objective optimization approaches are widely used by hydrological community (Harlin, 1991; Yapo et al., 1998; Liu et al., 2017, 2019; Pan et al., 2017; Shafii and Tolson, 2015). This set the stage of using some uncomprehensive but effective criteria as targets, such as aforementioned hydrological signatures (Shafii and Tolson, 2015; Westerberg and McMillan, 2015).

4

statistical targets and fractal criteria. Nonetheless, the strategy to use the Hausdorff dimension to calibrate hydrological models has not been studied.

In this study, a new criterion defined as ratio of fractal dimension (RD) is introduced, as well as a calibration strategy. The criterion and calibration strategy should be able to consider the self-affinity, periodicity, long-term memory and irregularity of hydrograph during model calibration. Three catchments with different climate and geography are used as case studies. The aim of this study is to examine the applicability of using RD as one of the targets of multi-objective calibration and explore the performance of hydrological models when RD is considered. Section 2 describes differences between RD and classical criteria, and how RD is used in calibration (E-RD strategy). Section 3 contains the brief information of study areas and methods used in this study to investigate the advantages of RD. Section 4 provides the results and Section 5 provides the discussion. Section 6 is the summary and conclusion. In this study, our goal is to answer the following questions: (1) Is RD a proper criterion for hydrological modelling, even if the reflection of RD is not as direct as classical criteria? (2) Could E-RD strategy explicitly improve the performance of hydrological models? (3) Why can RD be used to improve calibration?

2 Study area and methodology

2.1 Ratio of fractal dimensions and E-RD strategy

The box-counting method used to calculate the Hausdorff dimension is based on the idea of separating data into boxes and count the number of boxes (Mandelbrot, 2004). When adopted to analyze time series, the box-counting method sums adjacent data up (put adjacent individuals into boxes) and compares the treated data of various resolutions (different sizes of boxes). Fig. 1 graphically shows how the box-counting method works with time series. Fig. 1 (a) shows how the number of boxes needed to cover all data (N) changes when the size of boxes changes (resolution, δ). Fig. 1 (b) shows the log-linear relationship between N and δ. The definition of the Hausdorff dimension D is:

$$D = \frac{\log (N)}{\log (1/\delta)}; \tag{1}$$

Where δ is the size of boxes and N is the number of boxes (Evertsz and Mandelbrot, 1992).

5

移动了(插入) [2]

删除了: a

上移了 [3]: Chiew and McMahon (1993) classified into statistical parameters and dimensionless coefficients. Statistical parameters include mean value, standard deviation, coefficient of skewness, coefficient of variance and quantile points etc. Dimensionless coefficients include Pearson correlation coefficient (r^2), Nash-Sutcliffe efficiency coefficient (E) and Kling-Gupta efficiency coefficient etc. Most of the coefficients are based on the squared residuals (Pushpalatha et al., 2012). According to squared-residuals-based coefficients' calculation formula, approaching of every simulated individual data to observed data makes the coefficients better. However, this doesn't make models more convincing if the approaching of simulated individual data is against the physical feature of models and catchment. Another deficiency of existing criteria is the preference of

上移了 [4]: Following the fractal theory, descriptions of include the Hurst exponent (rescaled range analysis) (Hurst, 1951), Hausdorff dimension (box-counting dimension or

删除了: **2 Ratio of fractal dimension as a criterion of hydrological model calibration**
2.1 Existing criteria and their drawbacks … [3]

上移了 [5]: Generally, the Hausdorff dimension of streamflow series represents the magnitude of fluctuation, i.e., the fluctuations in river flow are large for large river

下移了 [6]: The value of Hausdorff dimension of the same time series may be different for different δ. The difference usually implicates that self-affinity of the time series changes

删除了: **2.3 Ratio of fractal dimensions**
The box-counting method used to calculate Hausdorff dimension is based on the idea of separating data into bo… [4]

上移了 [2]: Nonetheless, the strategy to use Hausdorff dimension to calibrate hydrological models has not been studied. The relevant examination of models' performance

删除了: analysis

删除了: of

设置了格式: 字体: 倾斜

设置了格式: 字体: 倾斜

Fig. 1. Flow chart of using box-counting method to calculate the Hausdorff dimension of time series.

As stated before, the observed and simulated streamflow series shall have the same Hausdorff dimension. In this study, a new criterion named as ratio of dimension (RD) is defined as follow:

$$RD = \frac{D_s}{D_o},\hspace{4cm}(2)$$

where D_s is the Hausdorff dimension of simulated streamflow series and D_o is the Hausdorff dimension of observed streamflow series. The range of RD is from 0 to $+\infty$. When RD=1, the simulated streamflow series has the same Hausdorff dimension with that of observed streamflow series, which means that the model is the best in terms of fractals. The relevant examination of models' performance under the supervision of RD has not been studied either.

Obviously, RD, as a metric of self-affinity deviation of simulated streamflow series from observed series, is not a criterion capable of evaluating the performance of hydrological models by itself. An immediate thought is to combine RD and another statistical criterion in model calibration.

Three features are demanded for the statistical criterion to be combined with RD. Firstly, the statistical criterion shall be able to evaluate the performance of models in terms of water balance to some extent. Secondly, the statistical criterion shall evaluate the response of streamflow to meteorological forcing. Thirdly, the criterion shall calculate model errors over the entire test period. These features make sure that the strategy meets basic needs. An additional requirement for the statistical criterion used in this study is the popularity of this criterion within the hydrological community. Therefore in this study, we choose E as the statistical criterion. Another reason to choose E is that the pros and cons of E are more familiar for hydrologists than other metrics, and this original version is still mostly often used in hydrological model calibration. In this manner, the advantages of RD emerge as well as the benefits of multi-objective calibration based on RD.

Nash-Sutcliffe efficiency coefficient (E), a commonly used criterion since initially proposed (Nash and Sutcliffe, 1970), is calculated is:

$$E = 1 - \frac{\sum(Q_o - Q_s)^2}{\sum(Q_o - \overline{Q_o})^2},\hspace{3cm}(3)$$

Where Q_s is the simulated flow, Q_o is the observed flow and $\overline{Q_o}$ is the mean value of the observed flow.

6

A set of experiments is processed to illustrate the benefits of using the proposed E-RD strategy to evaluate models. Descriptions of experiments are included in Section 3. Fig. 2 shows the whole process of E-RD strategy.

Fig. 2. Flow chart of E-RD strategy.

The value of Hausdorff dimension of the same time series may be different for different resolutions. The difference usually implicates that self-affinity of the time series changes as the resolution changes and in hydrology specifically, dominant driver of hydrological processes changes. For example, the dominant drivers of daily and annual circle of temperature are different. The Hausdorff dimension of joint data series (also called as joint multifractal spectrum) verifies the freezing-thawing process of soil moisture in a quantitative and solid way which unfolds the complex nonlinear relationship among three hydrological variables (Bai et al., 2019). According to this idea, the Hausdorff dimension determines whether the streamflow components are reasonably simulated. In this study, the largest temporal resolution is set as 365 days (1 year), to leave the inter-annual drivers out. It is believed that the range of resolution is enough for the Hausdorff dimension to reflect drivers of hydrological processes.

2.2 Study area

A small catchment located in Tibet named Dong, a medium sized catchment located in southeastern China named Jinhua and a large catchment located in the middle reach of Yangtze River named Xiang are used in this study.

Dong is a small tributary of the Yarlung Zangbo River, with elevations ranging from 3512 to 5869 m. The area of Dong catchment is about 43.6 km^2. The average annual precipitation of the study period is 413.5 mm. The average temperature is 10.6 ºC. The high elevation of Dong catchment results in cold climates. Former study has consolidated that snow pack and frozen soil significantly affect hydrological processes in the Dong catchment (Bai et al., 2019). Meteorological forcing data and streamflow observation of Dong catchment used in this study are from 2011 to 2014.

Jinhua River is a 5536-km^2 catchment of Zhejiang Province, southeastern China. The study area is

subject to Asian monsoon climate, and precipitation is strongly summer-dominant, occurring mostly from May to September. Based on meteorological data of 42 years (from 1965 to 2006), the mean annual precipitation in Jinhua catchment is 1847.4 mm. The average temperature is 17.6 ºC. Former

590 studies show that precipitation data and streamflow data of Jinhua catchment are well matched (Pan et al., 2018). Meteorological forcing data and streamflow observation of Jinhua catchment used in this study are from 1965 to 2006.

Xiang River is one of the largest tributaries of the Yangtze River, which flows into the Dongting Lake, the second largest freshwater lake in mid-China. The area of Xiang catchment is about 82,400 km^2

595 and data of nine meteorological stations are used in this study. Dominated by subtropical monsoon climate, the mean annual rainfall of the basin ranges from 1400 to 1700 mm and the average annual temperature is around 17 ºC. The basin experiences floods and droughts frequently, and rainfall is distributed evenly throughout the year, most of it falling in April to June. According to studies, precipitation is the most vital driver for Xiang River (Zhu et al., 2019). Meteorological forcing data

600 and streamflow observation of Xiang catchment used in this study are from 1987 to 2013.

Fig. 3 shows the topography of all study areas.

Fig. 3. DEM of study areas.

605

2.3 HBV model

The HBV model is a conceptual rainfall-runoff model originally developed by Swedish Meteorological and Hydrological Institute (SMHI) (Bergström, 1976; Bergstrom, 1992; Lindström et al., 1997). The model has been successfully used in many cases (Seibert and Vis, 2012; Tian et al.,

610 2015, 2016). The HBV model is composed of precipitation and snow accumulation routines, a soil moisture routine, a quick runoff routine, a baseflow routine and a transform function. The HBV model takes into account the effect of snow melting and accumulation, which is significant in the Dong catchment. The actual evapotranspiration is calculated with a linear function. Two conceptual runoff reservoirs, the upper reservoir and the lower reservoir are included in the HBV model.

8

删除了: (Pan et al., 2018)

设置了格式: 上标

删除了: literatures

删除了: (Zhu et al., 2019)

移动了(插入) [6]

删除了: The value of Hausdorff dimension of the same time series may be different for different δ. The difference usually implicates that self-affinity of the time series changes as the resolution changes and in hydrology specifically, dominant driver of hydrological processes changes. Hausdorff dimension helps reveal the dominant drivers of hydrological process (Bai et al., 2019). According to this idea, Hausdorff dimension determines whether the streamflow components are reasonably simulated. In this study, the largest temporal resolution is set as 365 days (1 year), to leave the inter-annual drivers out. It is believed that the range of resolution is enough for Hausdorff dimension to reflect drivers of hydrological processes.

删除了: 3

删除了: 2

删除了: The HBV model is a conceptual rainfall-runoff model originally developed by Swedish Meteorological and Hydrological Institute (SMHI) (Bergström, 1976; Bergström, 1992; Lindström et al., 1997). The HBV model has been successfully used in many cases (Seibert and Vis, 2012; Tian et al., 2015; Tian et al., 2016). The HBV model is composed of precipitation and snow accumulation routines, a soil moisture routine, a quick runoff routine, a baseflow routine and a transform function. The HBV model takes into account the effect of snow melting and accumulation, which is significant in the Dong catchment. In this study, the HBV model utilized is provided by Tian et al. (2015), compiled with MATLAB.

The HBV model has 14 parameters to control all above-mentioned hydrological processes. A simple description of seven parameters mentioned later is given here.

The runoff generation routine (response function) of HBV model transforms excess water from the soil moisture zone to runoff. The function consists of one upper, non-linear reservoir and one lower, linear reservoir, presenting fast ... [5]

2.4 Multi-objective genetic algorithm

A controlled and elitist genetic algorithm (a variant of NSGA-II) (Deb, 2001) is applied in model
calibration. A controlled and elitist GA favors individuals with better fitness value (rank) as well as
individuals that can help increase the diversity of the population even if they have a lower fitness
value. An important behavior of this genetic algorithm is that, the individual with the best performance
according to anyone of the criterion would be retained with the lowest rank. This makes sure that with
multi-objective genetic algorithm, parameter set with the best possible E could be found and the
following comparison between $RD\text{-}E$ and E is reasonable. In this study, $|1 - RD|$ is used as one
of the criteria.

Since HBV has 14 parameters to calibrate, the number of generations is 2800. Each generation has
600 population. The crossover fraction is set as 0.8 (meaning). The Pareto fraction is set as 0.2
(meaning). The population migrates every 20 generations, and the migration fraction is set as 0.5.
These settings make sure that population will not trap in local optimum, which is important because
RD varies in a wider range than traditional criteria. Most of these numbers are the default settings,
which is applicable to most of the problems. Only the number of the population of each generation
(600) is larger than default (200) for finer presentation of Pareto front of the optimization. The
meanings of settings can be found in Deb (2001).

All 600 Pareto-optimized solutions of the last generation are used in the following analysis. GA
optimization with the $E\text{-}RD$ calibration strategy (described in 2.1) will not drop population with
perfect RD (=1) and unsatisfactory E. Several representative selected parameter sets and
corresponding simulated streamflow series are deeply studied.

2.5 Approach for model evaluation

To investigate the RD's effects in hydrological model evaluation, several tools are utilized.
Pearson's correlation coefficient r^2, percentage bias (bias), auto-correlation of observation, auto-
correlation of simulation, relative variance, maximum monthly flow and minimum monthly flow are
used for a comprehensive comparison between models based on RD and traditional hydrological
criteria (E). The best RD model and best E model (typical models) are selected from the last
generation of GA calibration for detailed analysis.

9

To understand how the model is adjusted when RD is used as one of the objectives, the relationship between parameters and RD is analyzed. The distance correlation r_d^2 is used to determine whether the variations of model's parameters and RD are related. The distance correlation, as a multivariate measure of dependence, calculates the correlation of distances between points to means. The distance correlation is believed to have better performance when solving problems with non-linear data or extreme values (Székely et al., 2007). The relationship between parameters and RD may not be linear, which brings the necessity of using a nonlinear analysis approach rather than Pearson's linear correlation coefficient. Distance correlation is also more robust to data outliers, than rank correlations.

To look into the influence on simulation of specific parts of hydrographs brought by RD, fast flow and baseflow are analyzed separately. The HBV model is slightly modified to output simulated fast flow and baseflow at every time step. Observed streamflow series are divided into the fast and baseflow using the Water Engineering Time Series PROcessing tool (WETSPRO tool) introduced by (Willems, 2009). WETSPRO separates fast flow and slow flow on the basis of filter theory, using several filter parameters including recession constant and average fraction of fast flow volumes over the total flow volumes etc. The E and r^2 of simulated fast flow/baseflow to observed fast flow/baseflow are calculated. Hydrographs of the first three years after warming up are shown to visually illustrate the influence of RD on fast flow and baseflow simulation.

3 Results and discussion

3.1 Overall evaluation of models on the Pareto front

Fig. 4 shows the RD-E relationship of last population of multi-objective calibration in three catchments separately. The ranges of RD of final generation in three cases are different, so as the ranges of E/bias. The ranges of E are 0.60 to 0.69 (Dong), 0.95 to 0.953 (Jinhua) and 0.818 to 0.822 (Xiang). For all cases, the non-significant variation of E indicates that for all selected parameter sets, the E criteria could not fully distinguish them. On the contrary, the ranges of RD are about 0.72 to 1 (Dong), 0.86 to 1.04 (Jinhua) and 0.85 to 1.01 (Xiang). According to relevant studies, the biggest difference of Hausdorff dimension of data of the same type is smaller than 0.25 (Hurst, 1951; Rubalcaba, 1997; Meseguer-Ruiz et al., 2019), which indicates the ranges of RD aforementioned

10

删除了: hydrological

删除了: William (2009)

删除了: ,

删除了: ,

删除了: 4

删除了: 4

删除了: 1+2.8×10^{-12}

删除了: literatures

present the significant difference of simulated streamflow from the aspect of fractal. In this study, RD is often lower than 1 and sometimes only slightly higher than 1, which agrees with the smooth hydrograph and simple structure of HBV model. Because that RD=1 means that the model is best in terms of fractals (see Section 2.2), the models whose RD is larger than 1 need discussion, too. Noting that the largest RD is very close to the best RD (=1), the largest RD model should be similar with the best RD model. And the GA algorithm discards most of the models with $RD > 1$ because they are not on the Pareto front. The bias does not change much when RD changes. A tiny difference within 3% occurs for the last generations of Dong, Jinhua and Xiang. More importantly, change of bias with the change of RD is different for three cases. For Dong catchment, the bias is firstly getting worse then getting better as RD approaching 1. Besides, a trend of bias of getting worse for Jinhua and a trend of bias of getting better for Xiang as RD approaching 1 can be observed. Without more cases, the trend of bias in this study is regarded to be random. In addition, in Xiang case, there is a break in Fig. 4. On two sides of the break, E is close by and RD is significantly different.

A single-objective calibration is operated to support the assumptions made in Section 3.3 that, in this study, the NSGA II algorithm can find the best E. The comparison between results of single-objective calibration and multi-objective calibration (E-RD strategy) is listed in Table 1. Besides, to get rid of the possible influence of the lengths of time series, a comparison of the multi-objective calibration with the same length of data is made. The results show that, at least in the cases of this study, the E-RD strategy would not change its behavior with the lengths of data.

Fig. 4 E-RD of last generation of GA calibration.

Table 1. Comparison of best E between single-objective calibration and multi-objective calibration (E-RD strategy).

The models with the best RD, best E and largest RD are selected from the Pareto front as typical examples. Fig. 5 is the simulated streamflow of three examples and observed streamflow as well. For each case, discharge within a three-year period is shown. Examples with the largest RD are used to

删除了: are significant

删除了: can

删除了: '

删除了: was

删除了: could

verify if the model with the same RD with observation is the best. Apparently, the simulated hydrographs of typical models in each case are similar, which agrees with the E and RD in Fig. 4.

810

Fig. 5. Typical examples with best RD, best E and largest RD (representative three-year hydrograph).

A precondition of adopting the RD-E strategy is the irrelevancy or weak correlation between two

815 criteria. This precondition could be simply verified by looking into their calculation schemes or by examining during the multi-objective calibration. In this study, the calculation of two metrics (RD and E) are totally different, and the results of multi-objective calibration also show that the significant change of RD only leads to minor difference of E (see Fig. 4). The best E and worst E are close according to the result of multi-objective calibration. Figs. 4 and 5 further imply that only little

820 decrease of E happens when pursuing better RD. In this study, the equifinality of using only E emerges.

Table 2 lists the E values of typical models selected by the E-RD calibration strategy and optimized model. Table 2 confirms the assumption that, in this study, directly analyzing the models calibrated by E-RD calibration strategy is reasonable and efficient. Hydrological signatures including relative

825 variance, lag-1 auto-correlation, percentage bias and maximum/minimum monthly flow are used to show the effect of RD.

Table 2. Hydrological signatures of typical models in all three cases.

830 Table 2 shows the hydrological signatures of observed and simulated flow series in three cases. Most hydrological signatures, including lag-1 auto-correlation, relative variation and maximum monthly flow, of simulated series are close by. Lag-1 auto-correlations of simulated series are close with auto-correlations of observed flow series. The lag-1 auto-correlations of series of flow series in Dong case and Xiang case are more than 0.9 while the values in Jinhua case are between 0.75 to 0.77. The relative

835 variances of flow series in Dong case and Xiang case are smaller than 1, while the values in Jinhua

case are more than 1.8. These show the feature of catchments of different types which are well simulated by the HBV model. Maximum and minimum monthly flows of simulated and observed series are significantly different. In all three cases, maximum monthly flows of simulated series are close to each other and slightly smaller than maximum monthly flows of observed flow series. Minimum monthly flow is the only hydrological signature used in this study that distinguishes the typical models with the best RD and with the best E. In all three cases, the minimum monthly flow of simulated series with the best E is significantly smaller than of the minimum monthly flow observed series. On the contrary, the minimum monthly flow of simulated series with the best RD is close to the minimum monthly flow of observed series in Jinhua and Xiang cases. The minimum monthly flow of simulated series with the largest RD is worse than that of simulated series with the best RD. The high-flow percentiles (Q_5) and low-flow percentiles (Q_{75}) are reasonable in three cases for all typical models. However, the high-flow percentiles and low-flow percentiles of best RD models are still closest to the observation. In summary, hydrological signatures illustrate that major effects of RD are on the model's low flow simulation. Therefore, in later sections, low flow related analysis will be more emphasized.

3.2 Effect of RD on model parameters

All parameter sets in the Pareto front of three cases vary. The distance correlations (r_d^2) of parameters and RD are used to determine whether the change of parameters is stable. In addition, high value of r_d^2 indicates the significant relationship between the Hausdorff dimension and these parameters. In this study, the relation between GA-selected parameter sets and E is not shown because E and RD in the Pareto front are highly related and the variance of E is small (see Fig. 4).

Table 3 lists the determinative parameters of three cases respectively. Distance correlation (r_d^2) is used to illustrate the non-linear relationship between E and RD in the Pareto's optimal. The parameter effective precipitation exponent (β) and degree-day factor are also listed in Table 3. Effective precipitation exponent is listed in Table 3 because of two reasons: 1) the range of r_d^2 of β in Jinhua case is from 0.709 to 0.739 in Xiang case, which is better than all unlisted parameters; 2) β, as well as determinative parameters α, KF, KS, is a runoff-generation-related parameter. The degree-day factor is listed in Table 3 because of two reasons: 1) distance correlation between the degree-day factor

13

删除了: 4

删除了: ier

删除了: In this study, a value 0.8 of r_d^2 is used as the threshold of being determinative.

删除了: The parameters with $r_d^2 < 0.8$ in all cases are not listed in Table 3

875 and RD is close to 0.8 in Xiang case; 2) in Dong case, distance correlation analysis does not show the significance of ablation of snow to hydrograph. Capillary transport is not determinative parameters to RD in Dong and Jinhua and therefore no further discussion of them is given afterwards. The r_d^2 of β (0.512) in Dong catchment is smaller than those in other cases. Fig. 6 shows the relationship between β and RD.

880

Table 3. Determinative parameters and distance correlations (r_d^2) between parameters and RD.

*: $r_d^2 \geq 0.8$

885 Fig. 6. β and RD relationship in three cases.

An explicit relationship between parameters and criteria confirms that the effect of RD is not random. Six parameters (β, α, fast flow factor, baseflow factor, percolation, degree-day factor) are selected by distance correlation analysis for further discussion.

890 Fig. 7 shows the relationship between α and RD. The fast flow factor (KF) is related to RD in all cases. Fig. 8 shows the relationship between KF and RD. The varying patterns of α and KF are the same in three cases. The fast flow exponent α increases when RD approaches to 1 and KF decreases when RD approaches to 1.

895 Fig. 7. α and RD relationship in three cases.

Fig. 8. KF and RD relationship in three cases.

Fig. 9 shows how fast flow changes with different surface water storages under different KF and α
900 of example models with best RD and best E. For all cases, E selects higher KF and lower α. In Dong case, the relative difference of fast flow generation between best RD model and best E model is always around 36%. The difference of fast flow between best RD model and best E model is

删除了: The r_d^2 of α and RD is larger than 0.740 in all cases. …

删除了: KF

删除了: KF

删除了: α

删除了: KF

删除了: α

significant in Dong case for the whole simulated period. In Jinhua case, the relative difference between the best RD model and best E model decreases from more than 20% to less than 5%. In Xiang case, the relative difference between the best RD model and best E model decreases from about 16% to 8%. The difference between the best RD model and best E model is important during the dry period and reduces as water storage of upper reservoir increases (the wet period). The relative difference is greater in Jinhua case than in Xiang case in low flow periods but smaller in Jinhua case in high flow periods. That difference between the best E model and best RD model will finally lead to the greater variation of fast flow in low flow periods than in high flow periods. There are break points in Xiang case (Fig. 6, 7 and 8), but no evident effects shown in Fig. 5 and 9.

Fig. 9. Response of fast flow to surface water storage. For each case, fast flow responses of typical models with best RD and E are presented.

The baseflow (slow flow) factor (KS) is related to RD in all cases. Fig. 10 shows the relationship between KS and RD. The varying patterns of KS are the same in three cases. However, the variation ranges of KS in three cases are different. The largest value of KS in Dong (0.153) is much larger than that in Jinhua (0.063) and in Xiang (0.048). The smallest value of KS in Dong (0.016) is also larger than that in Jinhua (0.005) and in Xiang (0.010). The KS of best-E in the three cases follows the sequence of catchment area. This agrees with the regular pattern that the concentration time of slow flow is highly related with the area of catchment.

Fig. 10. KS and RD relationship in three cases.

The percolation is significantly related to RD in all cases. The range of percolation in Dong case is larger than the others. Fig. 11 shows the relationship between percolation and RD in three cases. Percolation increases in Dong case and decreases in other two cases when RD increases. The range of percolation in Dong is larger than in the others. KS and percolation determine the way HBV models baseflow. The percolation in Dong case is larger than the others, which is the reflection of

15

940 Dong catchment's arid climate. The percolation in Jinhua case is larger than the percolation in Xiang case, because the slope in Jinhua catchment is larger.

Fig. 11. Percolation and RD relationship in three cases.

945 The degree-day factor is significantly related to RD in Xiang case. However, the relationship between the degree-day factor and RD in Dong and Jinhua is weak. Fig. 12 shows the relationship between the degree-day factor and RD. The degree-day factor of most selected models of Dong case is smaller than 0.05, indicating that these models barely have any snow-melt runoff. When $RD>0.9$, several models have degree-day factors larger than 7. When RD is around 1, the range of degree-day 950 factor is 8.18 to 11.76, indicating that RD somehow detects the snow-melt runoff in the hydrograph and makes the HBV model simulate the snow-melt runoff more reasonably. Notably, the RD-selected degree-day factor in Dong case is too large according to the guidance of HBV (1.5 to 4 mm/day, in Sweden) (HBV light version 2, user's manual), which may result from the unsuitable lumped model structure of HBV in rugged mountainous catchment.

955 The degree-day factors in all selected models of Jinhua are large, but the temperature in Jinhua is too high to have snow accumulation. The distance correlation between the degree-day factor and RD is weak in Dong and Jinhua case. The range of degree-day factor of most models in Xiang case is from 2.8 to 3.4. The range is small and so as the difference of snow-melt runoff of selected models. By checking the temperature series in the Xiang catchment, we find there are 61 days (out of 27 years) 960 when the average temperature is below 0°C. Actually, since the Xiang catchment is large, there are snow events somewhere in the catchment almost every year. The low temperature may be covered by averaging, but the E-RD strategy captured it and illustrated this by noticeable value of degree-day factor.

965 Fig. 12. Degree-day factor and RD relationship in three cases.

As illustrated in Fig. 7, 8, 10 and 11, the three runoff-generation-routine parameters, namely baseflow

16

删除了: (Seibert, 2005)

删除了: is

删除了: the

删除了: Besides, in Xiang case, only 61 of 9862 days have minus temperature

删除了: That is, although the r_d^2 of degree-day factor and RD in Xiang case is large, the snow-melt runoff in Xiang catchment is not influential.

factor (KS), fast flow factor (KF) and fast flow exponent (α), have the same change patterns in three cases, suggesting a consistent preference of RD in all cases. Fig. 9 shows the visual difference of fast flow caused by introducing RD. However, other parameters have different change patterns along with RD because of different features of catchments (Fig. 6 and 12). For example, the soil parameter β, as illustrated by Equation (6), redistributes the precipitation and divides it into effective precipitation and infiltration. β in Dong case and Xiang case increases and β in Jinhua decreases when RD is getting better.

3.3 Analysis of separated streamflow

Separated simulated and observed streamflow series further reveal how RD influences model calibration results. The simulated total flow is also separated with the WETSPRO tool to make the principle of separation of simulation and observation same. Table 4 lists the parameters of WETSPRO in three cases. The recession constants are close to each other. The w-parameter filter, representing the case-specific average fraction of the quick flow volumes over the total flow volumes, shows the difference. The w-parameter filter of Dong catchment is 0.14, smaller than the other catchments, meaning that baseflow only occupies less proportion of total flow in Dong, showing the catchment features of small area and high slope. Fig. 13 shows the correlation coefficients between simulated and observed fast flow/baseflow (r_f^2 and r_b^2) and Nash-Sutcliffe efficiency coefficient (E_f and E_b) of all population of last generation in three cases and their variation with RD. The observed fast flow and baseflow are separated from observed total flow using WETSPRO (William, 2009) (see Section 3.4). In Dong case, both r_b^2 and r_f^2 slightly decrease as RD approaching 1. However, the range of r_f^2 in Dong case is from 0.02 to 0.15 and the range of r_b^2 is from about 0.3 to 0.6, which means no correlation exists between simulated and observed fast flow and baseflow. The E_f and E_b in Dong case improve to 0.06 and 0.24 respectively. In Jinhua and Xiang cases, all models of last generation of GA simulate fast flow well. The r_f^2 and E_f value in Jinhua case are above 0.95 and 0.94. The r_f^2 and E_f in Xiang case are above 0.78 and 0.70. Surprisingly, there is still an evident improvement of fast flow simulation due to the application of RD. The major improvement is the performance in baseflow simulation. The values of criteria of baseflow simulation (r_b^2 and E_b) are improved from poor to satisfactory. In Jinhua case, r_b^2 is improved from less than 0.1 to more than 0.45 and E_b is

17

improved from -10 to about 0.38. In Xiang case, r_b^2 is improved from about 0.4 to 0.75 and E_b is improved from -6 to 0.51.

Fig. 13. Correlation coefficients and Nash-Sutcliffe efficiency coefficients on fast flow and baseflow respectively of models of last generation in three cases.

Fig. 14 and 15 show separated streamflow of typical models and observed streamflow to make a visible comparison of models based on E and models based on RD. Fig. 14 shows the fast flow and Fig. 15 shows the baseflow.

Fig. 14. Fast flow of typical models and observations (representative three-years hydrograph).

Fig. 15. Baseflow of typical models and observations (representative three-years hydrograph).

The fast flow response of the best RD model in Dong case matches well to observed fast flow. The recession of fast flow of the best RD model in Dong case is too fast and the stable value is nearly zero, which is in the contrast of observation. The fast flow response of best E model in Dong is late, the recession of fast flow is too slow and fast flow at recession periods is too much. The fast flow response of largest RD model in Dong is also late, but the fast flow recession is more reasonable. In Jinhua and Xiang cases, simulated fast flow of all typical models well matches the observation. In all cases, the fast flow of best RD model is smaller than that of best E model and the difference is greater in low flow periods, which is consistent with Fig. 9.

In all three cases, the best RD models simulated baseflow well. RD selected models accurately simulated the seasonal flow variation of three catchments. The amplitude of baseflow fluctuation is close to separated observation by WETSPRO. The discharge also fits separated observation well. In all three cases, the best E models do not simulate the baseflow well enough. The models with the largest RD in three cases have different performance. Largest RD model in Dong case, of which $r_b^2 = 0.82$ and $E_b = 0.25$, is not satisfactory. On the contrary, r_b^2 and E_b of the best E model in

Dong are 0.87 and 0.79 respectively. The best E models in Jinhua and Xiang case, however, are close to the best RD models. According to Fig. 10 and 11, in Jinhua and Xiang cases, smaller KS and percolation (of best RD model) make smaller recharge and outflow (baseflow) of lower reservoir and smaller fluctuation of baseflow. In Dong case, bigger percolation increases the recharge and total baseflow and smaller KS extends the period of baseflow recession, making simulated baseflow more consistent with observation (Fig. 15).

Two reasons exist for the unsatisfactory simulation of fast flow in Dong case. The first one is that the HBV model is not capable of accurately simulating mountainous catchment with snowpack and little gauge data are available for the Dong catchment. The second one is that WETSPRO may fail to correctly separate the short streamflow series of Dong catchment. This needs to be further verified.

Another visual demonstrator of the preference of RD is Fig. 14 and 15. Fast flow generation based on RD is more immediate while baseflow generation based on RD is smoother. Both of them are visually better than that when RD is not taken into account.

Above results reveal the benefits of using RD and the slight decrease of E. The selection principle based on multi-objective calibration is therefore suggested following two steps: 1) sieving out all parameter sets whose RD is around 1 (in this case, considering the data precision of MATLAB, RD =1); 2) Choosing the parameter set with best E among the sets in Step 1. It is determined that the E-RD strategy using this selection principle improves the reliability of streamflow components simulation.

That is, RD selects responsive fast flow (confirmed in Fig. 14) and smooth baseflow (confirmed in Fig. 15) in all cases.

4 Conclusion

This study targeted at examining the possibility of using fractal theory to improve the performance of hydrological models. The definition of ratio of fractal dimension (RD) was proposed and used as a fractal criterion (against traditional statistical criteria). A scheme which combined RD and Nash-Sutcliffe efficiency coefficient (E) to calibrate hydrological models was developed and examined. Three study cases named Dong, Jinhua and Xiang were included in the examination. This is the first

删除了: to

删除了: simulate

删除了: '

删除了: **5**

time (to our best knowledge) that fractal theory was applied to calibrate hydrological models.

The main conclusions of this study are as follows:

1) The varying patterns of parameters of runoff generation routine (namely fast flow factor, fast flow exponent and baseflow factor) are similar in all cases of our study.

2) Several parameters were found to be related to RD. For instance, the E-RD strategy selected the degree-day factors with relatively high value in Dong case, which is not seen when only E was considered.

3. The E-RD strategy is innovative in hydrological modelling. That is, the E-RD calibration strategy is a potential way to take the fractality of observed streamflow series into consideration in model calibration. Since fractal (also regarded as self-affinity) widely exists in nature, the RD as a criterion can be a good supplement for hydrological model calibration.

The E-RD strategy introduced in this study needs more case studies to corroborate its capability further. The combination of other traditional statistical criteria and RD shall also be examined. More studies are also needed to dig out more benefits of applying fractal theory in hydrological modelling.

20

删除了: Here are t

删除了: found

删除了: in specific cases as a result of specific characteristics of study areas

删除了: and fractal of streamflow series is substantial

删除了: It's noted that t

删除了: here

1100 **Reference**

Bai, Z., Xu, Y.-P., Gu, H., and Pan, S.: Joint multifractal spectrum analysis for characterizing the nonlinear relationship among hydrological variables, J. Hydrol., 576, https://doi.org/10.1016/j.jhydrol.2019.06.030, 2019.

Bergstrom, S.: The HBV model-its structure and applications, 1992.

1105 Bergström, S.: Development and application of a conceptual runoff model for Scandinavian catchments, 1976.

Chiew, F. H. S. and McMahon, T. A.: Assessing the adequacy of catchment streamflow yield estimates, Soil Res., 31, 665–680, 1993.

Davis, A., Marshak, A., Wiscombe, W., and Cahalan, R.: Multifractal characterizations of

1110 nonstationarity and intermittency in geophysical fields: observed, retrieved, or simulated, J. Geophys. Res., 99, 8055–8072, https://doi.org/10.1029/94JD00219, 1994.

Deb, K.: Multi-objective optimization using evolutionary algorithms, John Wiley & Sons, 2001.

Demirel, M. C., Booij, M. J., and Hoekstra, A. Y.: Effect of different uncertainty sources on the skill of 10 day ensemble low flow forecasts for two hydrological models, Water Resour. Res., 49, 4035–

1115 4053, https://doi.org/10.1002/wrcr.20294, 2013.

Evertsz, C. J. G. and Mandelbrot, B. B.: Self-similarity of harmonic measure on DLA, Phys. A Stat. Mech. its Appl., 185, 77–86, 1992.

Falconer, K.: Fractal geometry: mathematical foundations and applications, John Wiley & Sons, 2004.

1120 Gao, Y., Leung, L. R., Zhang, Y., and Cuo, L.: Changes in moisture flux over the Tibetan Plateau during 1979–2011: insights from a high-resolution simulation, J. Clim., 28, 4185–4197, 2015.

Grassberger, P. and Procaccia, I.: Measuring the strangeness of strange attractors, Phys. D Nonlinear Phenom., 9, 189–208, 1983.

Gupta, H. V., Kling, H., Yilmaz, K. K., and Martinez, G. F.: Decomposition of the mean squared

1125 error and NSE performance criteria: Implications for improving hydrological modelling, J. Hydrol., 377, 80–91, https://doi.org/10.1016/j.jhydrol.2009.08.003, 2009.

Hao, Z. and Singh, V. P.: Entropy-Based Method for Bivariate Drought Analysis, J. Hydrol. Eng.,

18, 780–786, 2013.

Harlin, J.: Development of a process oriented calibration scheme for the HBV hydrological model, Hydrol. Res., 22, 15–36, 1991.

Hurst, H. E.: Long-term storage capacity of reservoirs, Trans. Amer. Soc. Civ. Eng., 116, 770–799, 1951.

Jain, S. K. and Sudheer, K. P.: Fitting of hydrologic models: a close look at the Nash–Sutcliffe index, J. Hydrol. Eng., 13, 981–986, 2008.

Jelinek: Automated detection of proliferative retinopathy in clinical practice, Clin. Ophthalmol., 2, 109, https://doi.org/10.2147/opth.s1579, 2008.

Katsev, S. and L'Heureux, I.: Are Hurst exponents estimated from short or irregular time series meaningful?, Comput. Geosci., 29, 1085–1089, https://doi.org/10.1016/S0098-3004(03)00105-5, 2003.

Kling, H., Fuchs, M., and Paulin, M.: Runoff conditions in the upper Danube basin under an ensemble of climate change scenarios, J. Hydrol., 424–425, 264–277, https://doi.org/10.1016/j.jhydrol.2012.01.011, 2012.

Krause, P., Boyle, D. P., and Bäse, F.: Comparison of different efficiency criteria for hydrological model assessment, Adv. Geosci., 5, 89–97, 2005.

Li, P., Zhang, Z., and Liu, J.: Dominant climate factors influencing the Arctic runoff and association between the Arctic runoff and sea ice, Acta Oceanol. Sin., 29, 10–20, 2010.

Lindström, G., Johansson, B., Persson, M., Gardelin, M., and Bergström, S.: Development and test of the distributed HBV-96 hydrological model, J. Hydrol., 201, 272–288, 1997.

Liu, L., Gao, C., Xuan, W., and Xu, Y.-P.: Evaluation of medium-range ensemble flood forecasting based on calibration strategies and ensemble methods in Lanjiang Basin, Southeast China, J. Hydrol., 554, 233–250, 2017.

Liu, L., Xu, Y. P., Pan, S. L., and Bai, Z. X.: Potential application of hydrological ensemble prediction in forecasting floods and its components over the Yarlung Zangbo River basin, China, Hydrol. Earth Syst. Sci., 23, 3335–3352, 2019.

Mandelbrot, B. B.: A fractal set is one for which the fractal (Hausdorff-Besicovitch) dimension

22

strictly exceeds the topological dimension, 2004.

Movahed, M. S. and Hermanis, E.: Fractal Analysis of River Flow Fluctuations (with Erratum), Phys. A Stat. Mech. Its Appl., 387, 915–932, 2008.

Nash, J. E. and Sutcliffe, J. V: River flow forecasting through conceptual models part I—A

1160   discussion of principles, J. Hydrol., 10, 282–290, 1970.

Onyutha, C., Rutkowska, A., Nyeko-Ogiramoi, P., and Willems, P.: How well do climate models reproduce variability in observed rainfall? A case study of the Lake Victoria basin considering CMIP3, CMIP5 and CORDEX simulations, Stoch. Environ. Res. Risk Assess., 33, 687–707, https://doi.org/10.1007/s00477-018-1611-4, 2019.

1165   Pan, S., Fu, G., Chiang, Y.-M., Ran, Q., and Xu, Y.-P.: A two-step sensitivity analysis for hydrological signatures in Jinhua River Basin, East China, Hydrol. Sci. J., 62, 2511–2530, 2017.

Pan, S., Liu, L., Bai, Z., and Xu, Y.-P.: Integration of remote sensing evapotranspiration into multi-objective calibration of distributed hydrology-soil-vegetation model (DHSVM) in a humid region of China, 10, 1841, https://doi.org/10.3390/w10121841, 2018.

1170   Pechlivanidis, I. G., Jackson, B., Mcmillan, H., and Gupta, H.: Use of an entropy-based metric in multiobjective calibration to improve model performance, Water Resour. Res., 50, 8066–8083, 2015.

Pushpalatha, R., Perrin, C., Moine, N. Le, and Andréassian, V.: A review of efficiency criteria suitable for evaluating low-flow simulations, J. Hydrol., 420–421, 171–182,

1175   https://doi.org/10.1016/j.jhydrol.2011.11.055, 2012.

Radziejewski, M, Kundzewicz, and ZW: Fractal analysis of flow of the river Warta, J Hydrol, 1997.

HBV light version 2, user's manual:

Seibert, J. and Vis, M. J. P.: Teaching hydrological modeling with a user-friendly catchment-runoff-model software package, Hydrol. Earth Syst. Sci., 16, 3315–3325, 2012.

1180   Shafii, M. and Tolson, B. A.: Optimizing hydrological consistency by incorporating hydrological signatures into model calibration objectives, Water Resour. Res., 51, 3796–3814, 2015.

Székely, G. J., Rizzo, M. L., and Bakirov, N. K.: Measuring and testing dependence by correlation of distances, Ann. Stat., 35, 2769–2794, 2007.

23

Tian, Y., Xu, Y. P., Booij, M. J., and Wang, G.: Uncertainty in future high flows in qiantang river

1185   basin, China, J. Hydrometeorol., 16, 363–380, https://doi.org/10.1175/JHM-D-13-0136.1, 2015.

Tian, Y., Xu, Y. P., Booij, M. J., and Cao, L.: Impact assessment of multiple uncertainty sources on

high flows under climate change, Hydrol. Res., 47, 61–74, 2016.

Westerberg, I. K. and McMillan, H. K.: Uncertainty in hydrological signatures, Hydrol. Earth Syst.

Sci., 19, 3951–3968, https://doi.org/10.5194/hess-19-3951-2015, 2015.

1190   Willems, P.: A time series tool to support the multi-criteria performance evaluation of rainfall-runoff

models, Environ. Model. Softw., 24, 311–321, 2009.

Yapo, P. O., Gupta, H. V., and Sorooshian, S.: Multi-objective global optimization for hydrologic

models, J. Hydrol., 204, 83–97, 1998.

Zhang, Q., Yu, Z. G., Xu, C. Y., and Anh, V.: Multifractal analysis of measure representation of

1195   flood/drought grade series in the Yangtze Delta, China, during the past millennium and their fractal

model simulation, Int. J. Climatol., 30, 450–457, https://doi.org/10.1002/joc.1924, 2010.

Zhou, Y., Zhang, Q., and Singh, V. P.: Fractal-based evaluation of the effect of water reservoirs on

hydrological processes: The dams in the Yangtze River as a case study, Stoch. Environ. Res. Risk

Assess., 28, 263–279, https://doi.org/10.1007/s00477-013-0747-5, 2014.

1200   Zhu, Q., Gao, X., Xu, Y. P., and Tian, Y.: Merging multi-source precipitation products or merging

their simulated hydrological flows to improve streamflow simulation, Hydrol. Sci. J., 64, 910–920,

https://doi.org/10.1080/02626667.2019.1612522, 2019.

1205

删除了: Abebe, N., A., Ogden, F., L. and Pradhan, N., R.: Sensitivity and uncertainty analysis of the conceptual HBV rainfall–runoff model: Implications for parameter estimation. J. Hydrol. 389(3-4): 301-310, 2010.

Bai, Z., Xu, Y. P., Gu, H. and Pan, S.: Joint multifractal spectrum analysis for characterizing the nonlinear relationship among hydrological variables. J. Hydrol., 576, 12-27, 2019.

Bergström, S.: Development and application of a conceptual runoff model for Scandinavian catchments. SMHI Report RHO NO. 7, Norrköping, Sweden, 1976.

Bergström, S.: The HBV model - its structure and applications. SMHI Reports RH NO. 4, Norrköping, Sweden, 1992.

Chang, T. P., Ko, H. H., Liu, F. J., Chen, P. H., Chang, Y. P., Liang, Y. H., Jang, H. Y., Lin, T. C. and Chen, Y. H.: Fractal dimension of wind speed time series. Appl. Energ., 93, 742-749, 2012.

Chiew, F., H., S. and McMahon, T., A.: Assessing the adequacy of catchment streamflow yield estimates. Soil Res. 31(5), 665-680, 1993.

Davis, A., Marshak, A., Wiscombe, W. and Cahalan, R.: Multifractal characterizations of nonstationarity and intermittency in geophysical fields: Observed, retrieved, or simulated. J. Geophys. Res.: Atmospheres, 99(D4), 8055-8072, 1994.

Deb, K.: Multi-Objective Optimization Using Evolutionary Algorithms. Chichester, England: John Wiley & Sons, 2001.

Demirel, M., C., Booij, M., J., and Hoekstra, A., Y.: Effect of different uncertainty sources on the skill of 10-day ensemble low flow forecasts for two hydrological models. Water Resour. Res. 49(7), 4035-4053, 2013.

Falconer, K.: Fractal geometry: mathematical foundations and applications. John Wiley & Sons, 2004.

Gao, Y., Leung, L., R., Zhang, Y. and Cuo, L.: Changes in moisture flux over the Tibetan Plateau during 1979–2011: insights from a high-resolution simulation. J. Climate, 28(10), 4185-4197, 2015.

Grassberger, P. and Procaccia, I.: Measuring the strangeness of strange attractors. Physica D: Nonlinear Phenomena, 9(1-2), 189-208, 1983.

Gupta, H.V., Kling, H., Yilmaz, K.K. and Martinez, G.F.: Decomposition of the mean squared error and NSE
... [6]

Table 1: Comparison of best *E* between single-objective calibration and multi-objective calibration (*E-RD* strategy).

	Single-objective (*E*)	Multi-objective (*E*)
Dong	0.696	0.690
Jinhua	0.951	0.953
Xiang	0.820	0.822

带格式的: 居中

带格式的: 居中

带格式的: 居中

带格式的: 居中

1305 **Table 2: Hydrological signatures of typical models in all three cases.**

		Observation	Best_RD	Best_E	Largest_RD
Auto correlation	Dong	0.97	0.99	1.00	1.00
	Jinhua	0.76	0.76	0.76	0.75
	Xiang	0.94	0.95	0.94	0.94
Relative variance	Dong	0.53	0.56	0.58	0.57
	Jinhua	1.87	1.87	1.87	1.89
	Xiang	0.99	0.82	0.92	0.92
Maximum monthly flow (m^3/s)	Dong	1.54	1.40	1.42	1.39
	Jinhua	531.19	497.40	503.68	496.77
	Xiang	4210.01	3956.24	4027.68	4042.94
Minimum monthly flow (m^3/s)	Dong	0.44	0.30	0.27	0.26
	Jinhua	60.64	58.85	50.45	60.19
	Xiang	961.00	975.07	812.02	840.02
High flow percentiles (Q_5)(m^3/s)	Dong	1.93	1.44	1.49	1.38
	Jinhua	752.00	745.02	734.12	740.28
	Xiang	6048.50	5817.06	5586.92	5817.08
low flow percentiles (Q_{75})(m^3/s)	Dong	0.50	0.39	0.40	0.38
	Jinhua	37.77	38.55	37.80	37.31
	Xiang	803.75	790.95	845.76	744.52

格式化表格

删除了: ↵

... [7]

26

Table 3: Determinative parameters and distance correlations (r_d^2) between parameters and *RD*. *: $r_d^2 \geq 0.8$

	r_d^2 (range of parameter)		
	Dong	Jinhua	Xiang
Effective precipitation exponent (β) (mm/mm)	0.363 (0.010~0.012)	0.709 (0.791~0.911)	0.739 (0.435~0.499)
Fast flow exponent (α)	0.383 (0.100~0.124)	*0.808 (0.473~0.579)	0.734 (0.677~0.819)
Fast flow factor (*KF*)	*0.853 (0.002~0.005)	*0.812 (0.031~0.056)	*0.823 (0.003~0.006)
Baseflow factor (*KS*)	*0.932 (0.016~0.153)	*0.922 (0.005~0.063)	*0.950 (0.010~0.048)
Percolation (mm/day)	*0.879 (1.37~7.00)	*0.841 (1.10~2.34)	*0.959 (1.62~3.16)
Capillary transport (mm/day)	0.122 (0~0.035)	0.084 (3.84~4.00)	*0.914 (1.91~2.70)
Degree-day factor (mm/(day ℃))	0.117 (0.01~12.2)	0.171 (14.5~15.6)	*0.791 (2.80~4.20)

1310

27

Table 4 Parameters of WETSPRO.

Parameter	Dong	Jinhua	Xiang
Recession constant (days)	90	80	90
w-parameter filter	0.14	0.43	0.38

315
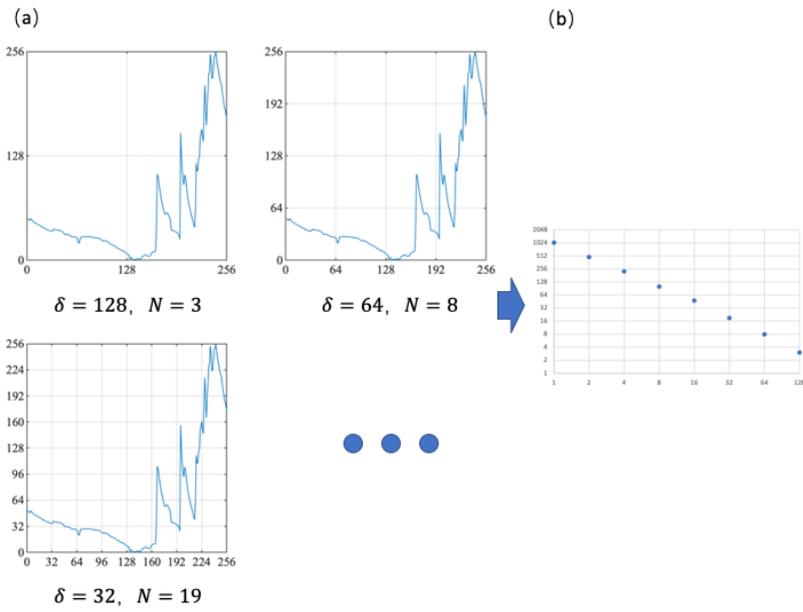
Figure 1: Flow chart of using box-counting method to calculate the Hausdorff dimension of time series.

1320
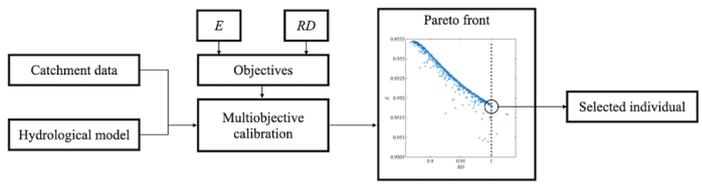
Figure 2: Flow chart of *E-RD* strategy.

1325
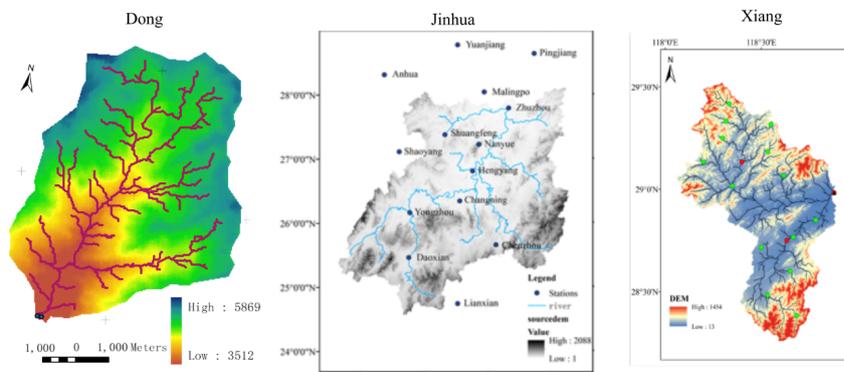
Figure 3: DEM of study areas.

1330
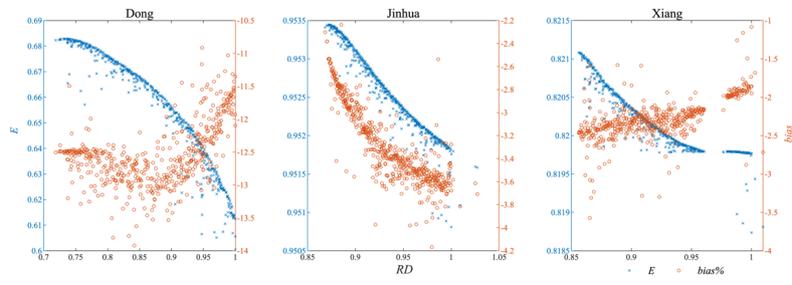
Figure 4：*E-RD* **of last generation of GA calibration.**

1335
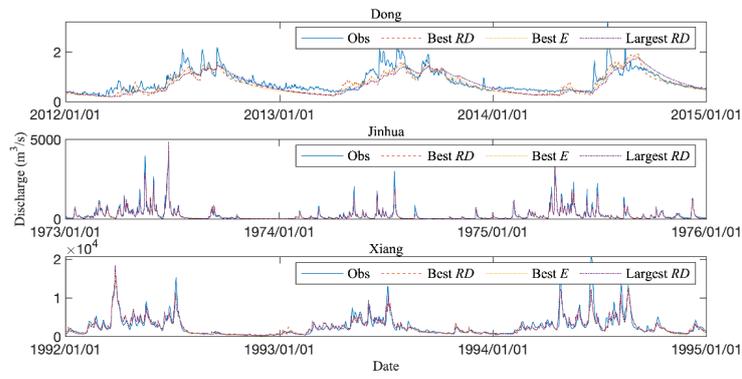
Figure 5: Typical examples with best *RD*, best *E* and largest *RD* (representative three-year hydrograph).

Figure 6: β and RD relationship in three cases.

1345   **Figure 7:** α and RD relationship in three cases.

删除了：
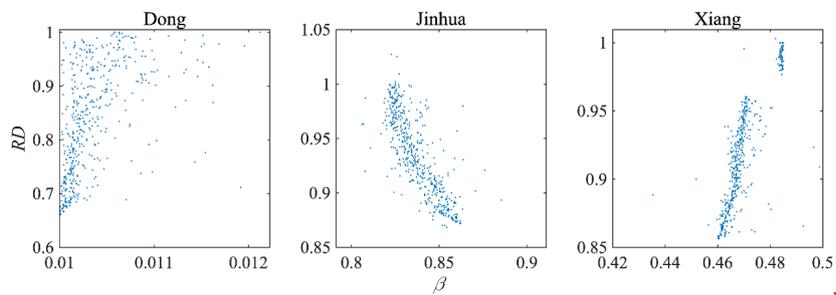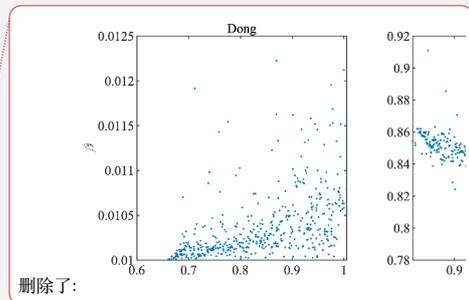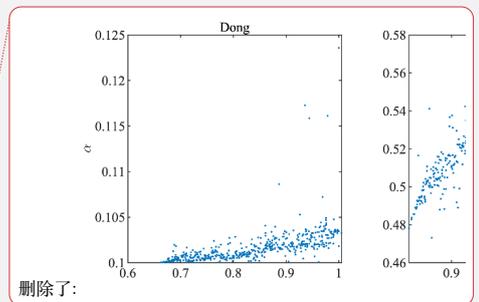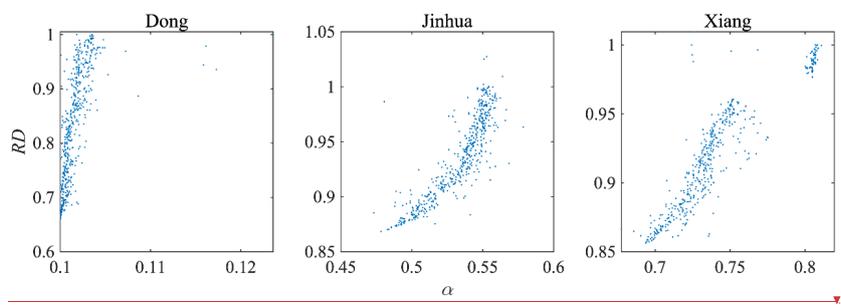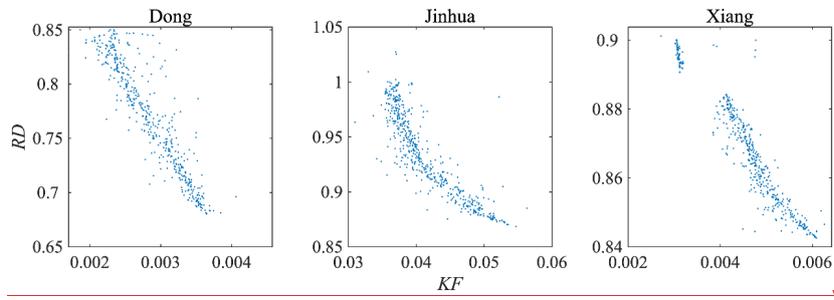
Figure 8: *KF* and *RD* relationship in three cases.
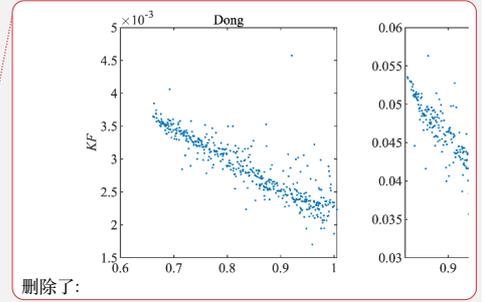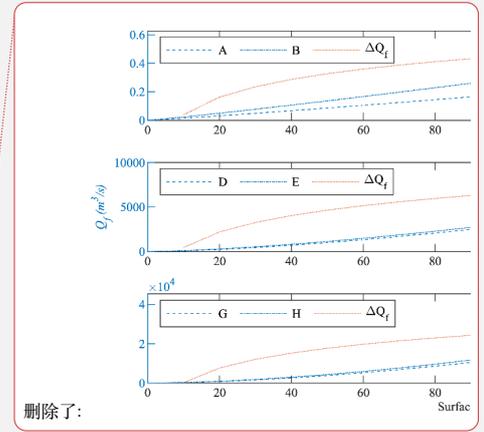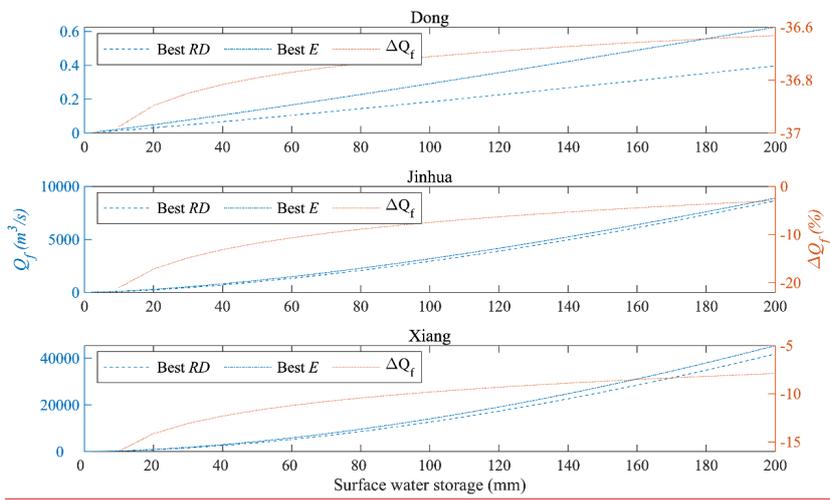
Figure 9: Response of fast flow to surface water storage. For each case, fast flow responses of typical models with best *RD* and *E* are presented.
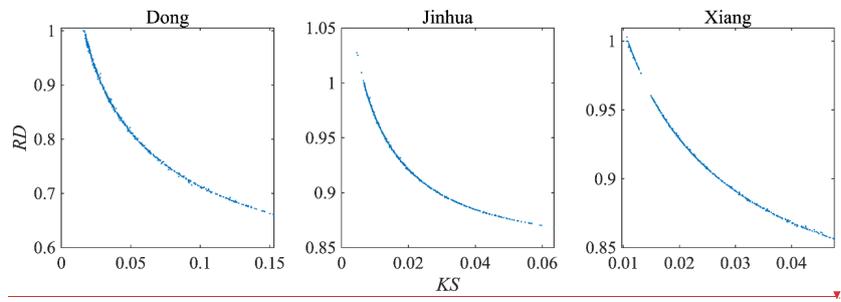
Figure 10: *KS* and *RD* relationship in three cases.

1360

38
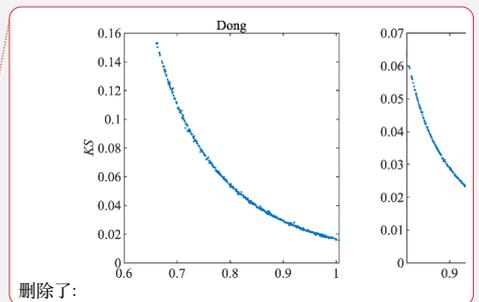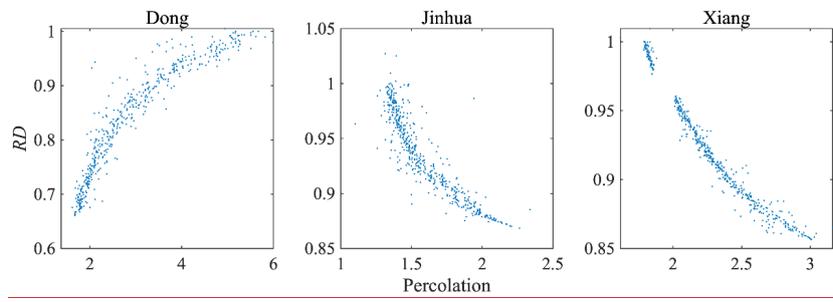
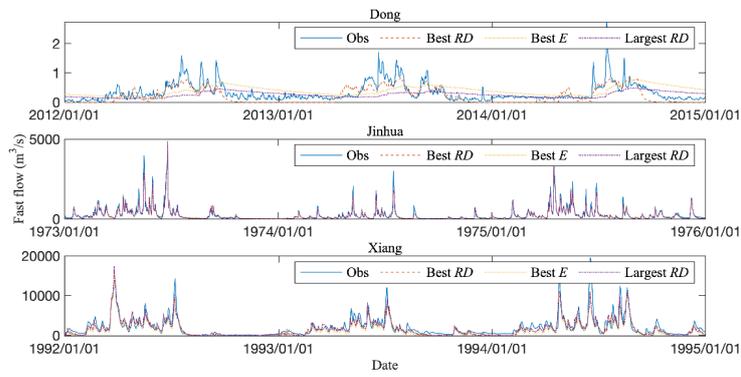**Figure 11: Percolation and *RD* relationship in three cases.**
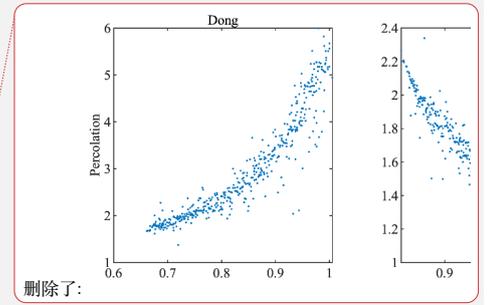
删除了:
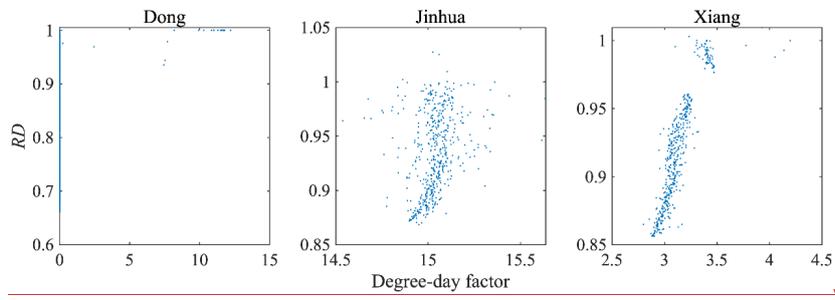
Figure 12: **Degree-day factor and** *RD* **relationship in three cases.**

删除了：
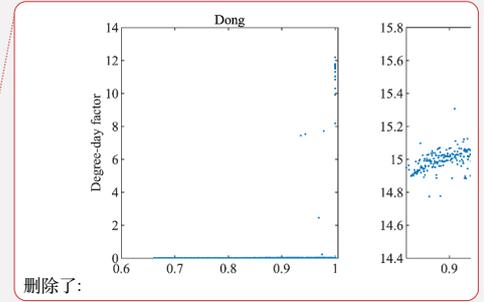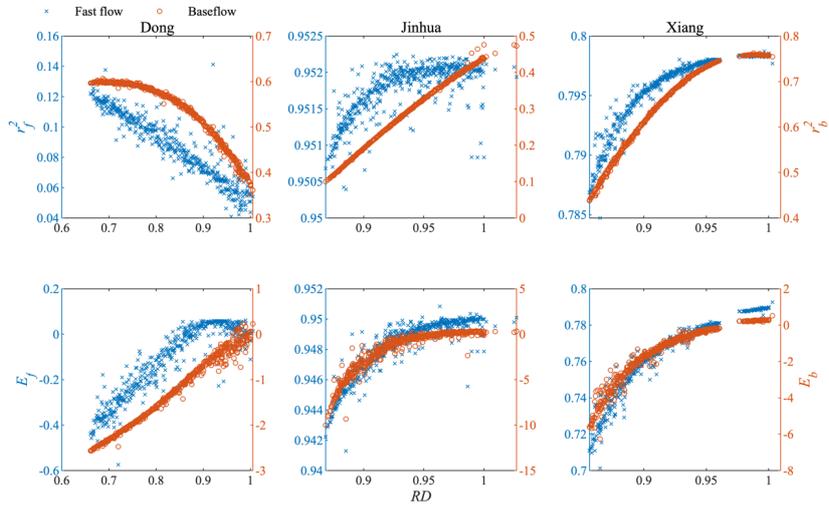
Figure 13: Correlation coefficients and Nash-Sutcliffe efficiency coefficients on fast flow and baseflow respectively of models of last generation in three cases.

1370

1375   **Figure 14: Fast flow of typical models and observations (representative three-years hydrograph).**
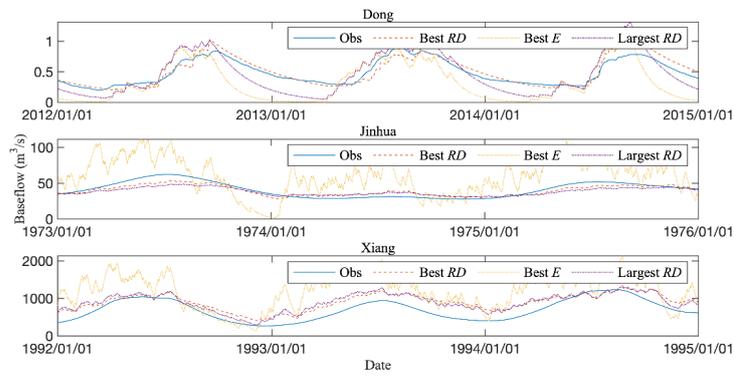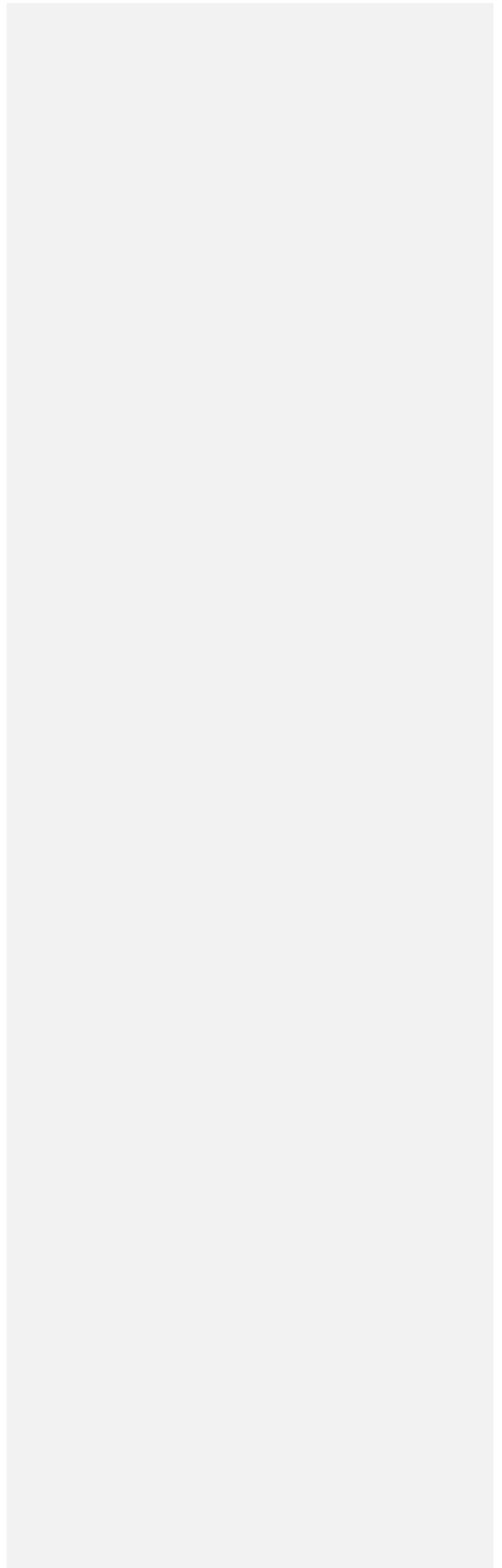
Figure 15: Baseflow of typical models and observations (representative three-years hydrograph).

删除了: Fig. 15.

43

第 2 页: [1] 删除了　　bai zhixu　　2021/2/20 PM4:15:00

第 2 页: [2] 删除了　　bai zhixu　　2021/2/13 PM8:36:00

第 5 页: [3] 删除了　　bai zhixu　　2021/2/13 PM5:25:00

第 5 页: [4] 删除了　　bai zhixu　　2021/2/13 PM5:17:00

第 8 页: [5] 删除了　　bai zhixu　　2021/2/13 PM8:04:00

第 24 页: [6] 删除了　　bai zhixu　　2021/4/24 PM1:30:00

第 26 页: [7] 删除了　　bai zhixu　　2021/2/13 AM10:42:00